Special Issue Article

Advances in Mechanical Engineering

Advances in Mechanical Engineering
2016, Vol. 8(5) 1–16

DOI: 10.1177/1687814016644377
aime.sagepub.com
SAGE

Generic control flow for the four types of clutch-to-clutch shifts

Yunjiang Cheng[1,2,3], Xiangyang Xu[1,2], Shuhan Wang[1,3] and Yang Liu[1]

Abstract

It is known that the clutch-to-clutch shifts in both planetary-type automatic transmission and dual clutch transmission can be divided into four types, which are power-on upshift, power-on downshift, power-off upshift, and power-off downshift. In previous studies, many control methods of clutch-to-clutch shifts are analyzed, but the control flows of the four types are different. In this article, the principle of these shifts is analyzed in detail. The concept of oncoming clutch's torque ability is proposed. A generic control flow is designed, which divides the shift processes of the four types into the same three phases, and the control algorithm in transmission control unit and the calibration process can be simplified. The powertrain system model and the shift controller are established on MATLAB/Simulink platform. The generic control flow is verified by software-in-the-loop simulations. The simulation results show that the proposed generic control flow can control the four types of shifts properly.

Keywords

Clutch-to-clutch shift, generic control flow, torque ability, automatic transmission, dual clutch transmission

Date received: 5 October 2015; accepted: 17 March 2016

Academic Editor: Nasim Ullah

Introduction

Among the several kinds of automatic transmissions (ATs), the planetary-type AT has a competitive relationship with the dual clutch transmission (DCT) in the automobile market. Both of them are stepped ATs and have the ability to realize a gearshift without torque interruption, which is known as a clutch-to-clutch shift. The AT have been developed more than 70 years, and the one-way clutches, which can automatically disengage if the input torque becomes negative, are used to realize clutch-to-clutch shifts in the early age. As the development of transmission control unit (TCU), more accurate control algorithms can be implemented and thus the clutch-to-clutch shifts can be realized without one-way clutches. The DCT emerges as the times require with high-performance TCU for better fuel economy compared to the AT. However, the dual mass fly wheel has to be equipped in DCT to isolate engine vibration from the transmission and drive train. In an AT, the vibration can be absorbed by a torque converter. For the same reason, the one-way clutches can be cancelled from AT to lower the cost, and the mechanical efficiency of AT can be improved by engaging the torque converter clutch after the vehicle start. In order to realize these, the research on the clutch-to-clutch shifts becomes very important.

[1]School of Transportation Science and Engineering, Beihang University, Beijing, China
[2]Beijing Key Laboratory for High-efficient Power Transmission and System Control of New Energy Resource Vehicle, Beihang University, Beijing, China
[3]National Engineering Research Center for Passenger Car Auto-Transmissions, Weifang, Shandong, China

Corresponding author:
Shuhan Wang, School of Transportation Science and Engineering, Beihang University, 37 Xueyuan Road, Haidian District, Beijing 100191, China.
Email: wsh@buaa.edu.cn

It is known that the clutch-to-clutch shifts in both AT and DCT can be divided into four types, which are power-on upshift, power-on downshift, power-off upshift, and power-off downshift. The shift processes of the four types can theoretically be divided into two phases which are torque phase and inertia phase. Many researches have been done on the clutch-to-clutch shifts. For the power-on upshift, the slide mode control is adopted by Runde[1] in both torque phase and inertia phase; an open-loop control based on randomized algorithms is proposed by Yoon and Khargonekar;[2] the optimal control based on the cost functions is used by Haj-Fraj and Pfeiffer;[3] Bai et al.[4] proposes a hydraulic wash-out technique to control the synchronization of the oncoming and the offgoing clutches; a robust adaptive scheme with intelligent supervision is used to reduce the shock and prevent an excessive slip by Kim et al.;[5] the close-loop control and output torque control are adopted by Goetz et al.;[6] the dynamic characteristics of the shift events of DCT are studied by Kulkarni et al.;[7] Dong et al.[8] investigates the pressure control of clutch for start stop function; and the vibration response during shift is analyzed by Walker and colleagues.[9,10] For the power-on downshift, the shift processes including engine torque control, clutch slip control, and transmission output torque control are designed by Goetz et al.;[11] shift control strategy and experimental validation in DCT are studied by Liu et al.;[12,13] and the constant output torque control technology based on a power-based integrated powertrain control system is developed by Bai et al.[14]

In previous researches, they mainly focus on the study of control methods for the torque phase and the inertia phase during the clutch-to-clutch shift process, and the control strategies for the power-on upshift and power-on downshift are often analyzed separately. Although the control principle of power-off downshift is similar to that of power-on upshift and the control principle of power-off upshift is similar to that of power-on downshift, rare research analyses the control strategies for the power-off downshift and the power-off upshift in detail. In this article, the concept of oncoming clutch's torque ability is proposed, and then a generic control flow (GCF) is designed to control all the four types of clutch-to-clutch shifts, which divides the shift processes into three same control phases.

This article starts with an overview of the dynamic model of the powertrain system. This is then followed by a principle analysis of the four types of clutch-to-clutch shifts. Then, the frame of the clutch controller is introduced. In the next section, the GCF for the four types of clutch-to-clutch shifts is described in detail. At the end of this article, the four types of clutch-to-clutch shifts have been simulated based on the GCF, and the three phases during each clutch-to-clutch shift is analyzed in detail. The conclusions are presented in the last section.

Dynamic model of the powertrain system

Powertrain structure

In order to study control algorithms for clutch-to-clutch shifts, the powertrain system model should be built appropriately. A low-order model can reduce the computational demand, but on the other hand it must be complex enough to reflect relevant dynamics of the powertrain system. Therefore, a 7 degree-of-freedom (DOF) powertrain model is developed in the research, which includes an engine model (1DOF), seven clutch models, a torque converter model (1DOF), a planetary model of 6AT (3DOF), a differential model, a tire model (1DOF), and a vehicle load model (1DOF) (Figure 1).

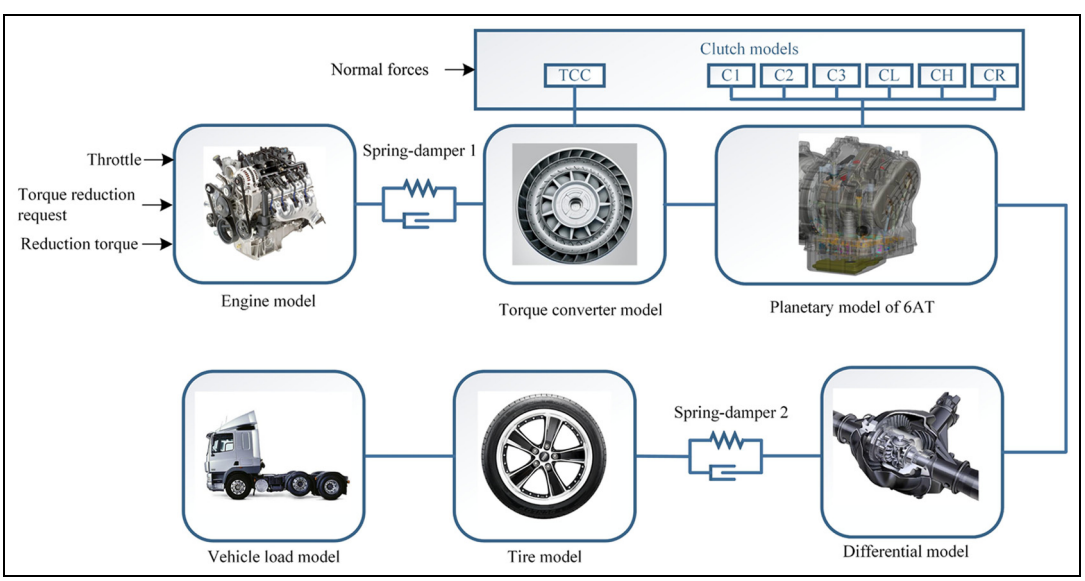

Figure 1. Outline of the powertrain dynamic model.

And the dynamic equations of the powertrain model are composed by the dynamic equations of those models.

Engine model

The engine map model is adopted considering the model complexity and computational demand. During the clutch-to-clutch shift process, the engine torque may need to be controlled for the synchronization of oncoming clutch speed. Therefore, if the torque reduction request is *True*, the reduction torque will be subtracted from the engine torque. For simplicity, the delay of torque response is modeled by a first-order damp element and is set to zero when the torque reduction request is *False*. The dynamic equation is as follows

$$I_e\ddot{\theta}_e - C_1(\dot{\theta}_p - \dot{\theta}_e) - K_1(\theta_p - \theta_e) = T_e - L^{-1}\left[\frac{L[T_{rt}]\cdot 1}{t_{rt}s + 1}\right] \tag{1}$$

where I_e is the engine inertia; θ_e and θ_p are the rotational displacement of engine and pump, respectively; K_1 is the equivalent stiffness coefficient of engine; C_1 is the equivalent damping coefficient of engine; T_e is the engine torque; T_{rt} is the reduction torque; t_{rt} is the time constant of engine torque response; s is the complex frequency; and L denotes the Laplace transform.

Clutch model

The powertrain system contains a torque converter clutch and six multi-disc clutches. Before the discussion of clutch models, three concepts need to be explained. The first is the "torque capacity," which is the maximum torque the clutch can transfer and be controlled by the normal force applied on the clutch plates; the second is "actual torque," which is the torque transferred by a clutch;[14] and the third is "drive torque capacity," which is the torque exerted on the drive shaft of a clutch (Figure 2).

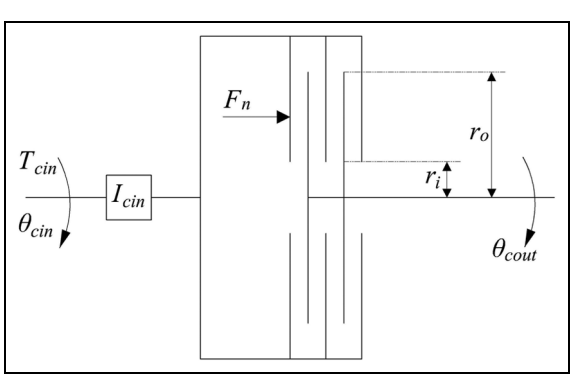

Figure 2. Sketch of a multi-disc clutch.

The torque capacity can be obtained from empirical formula[15,16] which is proportional to the normal force transferred by the clutch plates and the friction coefficient (equation (2))

$$T_{cc} = F_n \cdot \mu(\Delta\dot{\theta}_c) \cdot N \cdot \left(\frac{r_o^3 - r_i^3}{r_o^2 - r_i^2}\right) \tag{2}$$

According to the slip speed of the clutch, the calculation of actual torque can be divided into slip state and stick state (equations (3) and (4))

$$T_{ccd} = T_{cin} - I_{cin}\ddot{\theta}_{cin} \tag{3}$$

$$T_{ca} = \begin{cases} T_{cc} & \left|\Delta\dot{\theta}_c\right| \geq n_{eps} \text{ (slip state)} \\ \min(T_{ccd}, T_{cc}) & \left|\Delta\dot{\theta}_c\right| < n_{eps} \text{ (stick state)} \end{cases} \tag{4}$$

where T_{cc}, T_{ca}, and T_{ccd} are the torque capacity, actual torque, and drive torque capacity of a clutch, respectively; F_n is the normal force; $\mu(\Delta\dot{\theta}_c)$ is the friction coefficient; N is the number of friction surfaces; r_o is the friction surface outer radius; r_i is the friction surface inner radius; T_{cin} is the torque exerted on the input side; I_{cin} is the inertia of the input side; $\dot{\theta}_{cin}$ is the input-side speed; $\dot{\theta}_{cout}$ is the output-side speed; $\Delta\dot{\theta}_c$ is the slip speed, which equals to $\dot{\theta}_{cin} - \dot{\theta}_{cout}$; and n_{eps} is the critical slip.

The modeling challenge is how to handle the state change appropriately (slip state to stick state or stick state to slip state). The hyperbolic tangent function (or other similar functions) can connect the two states continuously (equation (5))

$$T_{ca} = T_{cc} \cdot \tanh\left(\frac{\Delta\dot{\theta}_c}{\alpha_c}\right) \tag{5}$$

where α_c is the scaling factor of the hyperbolic tangent function clutch model.

The hyperbolic tangent function clutch model is simple and easy to use, but it has a couple of minor problems. First, in order to carry torque, the clutch slip speed has to be non-zero. This means that there will be a small slip speed between the clutch plates when the clutch is in the stick state. Second, although this slip speed can be reduced using a small scaling factor, it could make the simulation model run slow or could make the model unstable.[14]

Another method is to build the slip state and the stick state separately. However, a variable step solver has to be chosen to find the critical slip, which is an approximation of zero such that numerical error in calculations is eliminated without negatively affecting results, including the stick-slip phenomenon. And thus the piecewise clutch model may not be suitable for real-time researches in which a fixed step solver is often chosen (Figure 3).

In this article, the piecewise clutch model is adopted for software-in-the-loop simulation in which a variable step solver ode15s is chosen. In the following research, the hyperbolic tangent function clutch model will be adopted for hardware-in-the-loop simulation in which a fixed step solver ode4 (Runge–Kutta) is chosen.

Torque converter model

The steady-state torque converter model is adopted, with torque ratio and K-factor data provided by the component supplier. The dynamic equations of the torque converter model are shown in equations (6)–(9)

$$I_p\ddot{\theta}_p + C_1(\dot{\theta}_p - \dot{\theta}_e) + K_1(\theta_p - \theta_e) = -T_p - T_{ctc} \quad (6)$$

$$T_p = \begin{cases} sign(1 - i_{tc}) \cdot [\dot{\theta}_p / K(i_{tc})]^2 & K(i_{tc}) \neq 0 \\ 0 & K(i_{tc}) = 0 \end{cases} \quad (7)$$

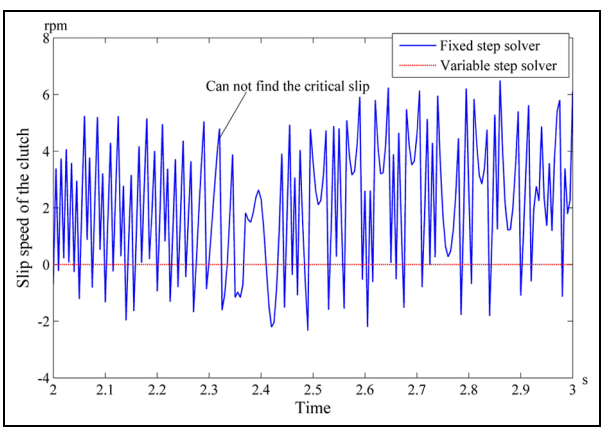

Figure 3. Comparison between a variable step solver and a fixed step solver.

$$i_{tc} = \frac{\dot{\theta}_1}{\dot{\theta}_p} \quad (8)$$

$$T_1 = T_p \cdot \alpha(i_{tc}) + T_{ctc} \quad (9)$$

where I_p is the pump inertia; T_p is the pump torque; T_1 is the turbine torque; T_{ctc} is the actual torque of torque converter clutch; i_{tc} is the speed ratio of torque converter; $K(i_{tc})$ is the K-factor of torque converter; θ_1 is the rotational displacement of turbine; and $\alpha(i_{tc})$ is the torque ratio of torque converter.

6AT planetary model

The 6AT contains two simple minus planetary gear sets and one compound planetary gear set (Figure 4). The Lagrange method is adopted to describe the dynamic model.

Equation (10) is the general form of Lagrange equations of the first kind for systems with linear speed constraints,[17] and equation (11) is the form of the linear speed constraint equations

$$\frac{d}{dt}\left(\frac{\partial L}{\partial \dot{\theta}_j}\right) - \frac{\partial L}{\partial \theta_j} - Q_j + \sum_{i=1}^{S} \lambda_i \frac{\partial f_i}{\partial \theta_j} + \sum_{i=1}^{r} F_i A_{ij} = 0 \quad (j = 1, 2, \ldots, m) \quad (10)$$

$$\sum_{j=1}^{m} A_{ij}(\theta_1, \theta_2, \ldots, \theta_m, t)\dot{\theta}_j + b_i(\theta_1, \theta_2, \ldots, \theta_m, t) = 0 \quad (i = 1, 2, \ldots, r) \quad (11)$$

where ∂ is the partial derivative; L is the Lagrange function; θ is the generalized coordinate; Q is the generalized non-potential force; F and λ are the Lagrange multipliers, also known as the internal forces; m is the number of generalized coordinates; S is the number of

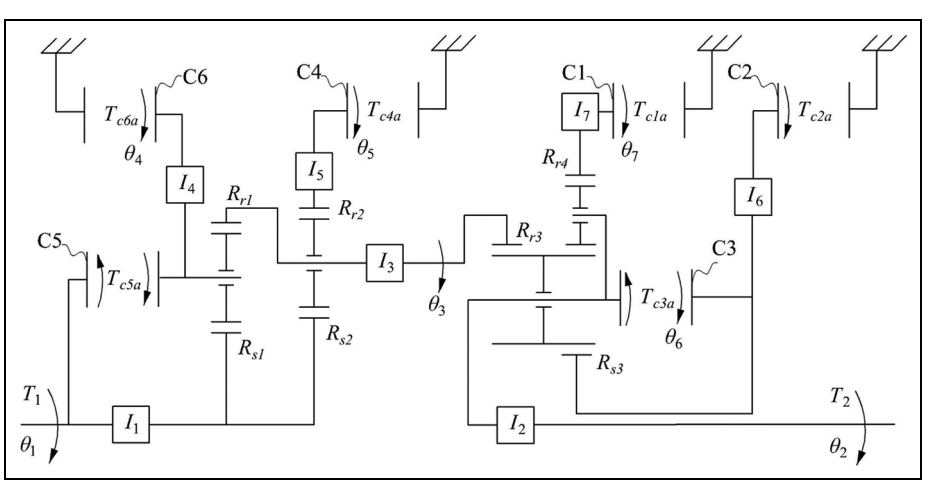

Figure 4. Structure of planetary system of 6AT.

constraint equations; and r is the number of linear speed constraint equations.

Under the condition of ideal constraint, four independent speed constraint equations of the system can be obtained (equations (12)–(15))

$$R_{s1} \cdot \dot{\theta}_1 + R_{r1} \cdot \dot{\theta}_3 = (R_{s1} + R_{r1}) \cdot \dot{\theta}_4 \tag{12}$$

$$R_{s2} \cdot \dot{\theta}_1 + R_{r2} \cdot \dot{\theta}_5 = (R_{s2} + R_{r2}) \cdot \dot{\theta}_3 \tag{13}$$

$$R_{s3} \cdot \dot{\theta}_6 + R_{r3} \cdot \dot{\theta}_3 = (R_{s3} + R_{r3}) \cdot \dot{\theta}_2 \tag{14}$$

$$-R_{s3} \cdot \dot{\theta}_6 + R_{r4} \cdot \dot{\theta}_7 = (R_{r4} - R_{s3}) \cdot \dot{\theta}_2 \tag{15}$$

where R_{si} is the radius of circle passing through the center of the ith sun gear; R_{ri} is the radius of circle passing through the center of the ith ring gear; and θ_i is the rotational displacement of the ith shaft (Figure 4).

According to equations (10)–(15), the dynamic equations of planetary system of 6AT can be obtained in matrix format (equation (16))

$$\mathbf{M} \cdot \mathbf{\Omega} = \mathbf{T} \tag{16}$$

Here

$$\mathbf{M} = \begin{bmatrix} I_1 & 0 & 0 & 0 & 0 & 0 & 0 & R_{s1} & R_{s2} & 0 & 0 \\ 0 & I_2 & 0 & 0 & 0 & 0 & 0 & 0 & 0 & -R_{s3} - R_{r3} & R_{s3} - R_{r4} \\ 0 & 0 & I_3 & 0 & 0 & 0 & 0 & R_{r1} & -R_{s2} - R_{r2} & R_{r3} & 0 \\ 0 & 0 & 0 & I_4 & 0 & 0 & 0 & -R_{s1} - R_{r1} & 0 & 0 & 0 \\ 0 & 0 & 0 & 0 & I_5 & 0 & 0 & 0 & R_{r2} & 0 & 0 \\ 0 & 0 & 0 & 0 & 0 & I_6 & 0 & 0 & 0 & R_{s3} & -R_{s3} \\ 0 & 0 & 0 & 0 & 0 & 0 & I_7 & 0 & 0 & 0 & R_{r4} \\ R_{s1} & 0 & R_{r1} & -R_{s1} - R_{r1} & 0 & 0 & 0 & 0 & 0 & 0 & 0 \\ R_{s2} & 0 & -R_{s2} - R_{r2} & 0 & R_{r2} & 0 & 0 & 0 & 0 & 0 & 0 \\ 0 & -R_{s3} - R_{r3} & R_{r3} & 0 & 0 & R_{s3} & 0 & 0 & 0 & 0 & 0 \\ 0 & R_{s3} - R_{r4} & 0 & 0 & 0 & -R_{s3} & R_{r4} & 0 & 0 & 0 & 0 \end{bmatrix} \tag{17}$$

$$\mathbf{\Omega} = [\ddot{\theta}_1 \quad \ddot{\theta}_2 \quad \ddot{\theta}_3 \quad \ddot{\theta}_4 \quad \ddot{\theta}_5 \quad \ddot{\theta}_6 \quad \ddot{\theta}_7 \quad F_1 \quad F_2 \quad F_3 \quad F_4]^T \tag{18}$$

$$\mathbf{T} = [T_1 - T_{c5a} \quad T_2 - T_{c3a} \quad 0 \quad T_{c5a} + T_{c6a} \quad T_{c4a} \quad T_{c2a} + T_{c3a} \quad T_{c1a} \quad 0 \quad 0 \quad 0 \quad 0]^T \tag{19}$$

where I_i is the inertia of the ith shaft; F_i is the internal forces of planetary gear sets; and T_{cia} is the actual torque of the ith clutch; T_1 is the input torque exerted on the turbine shaft; and T_2 is the load torque exerted on the output shaft of 6AT.

The other models

The differential is modeled as a simple connecting compound with the final ratio, and the non-rigid of the drive shafts is considered by a spring-damper element (equations (20) and (21))

$$\dot{\theta}_8 = \frac{\dot{\theta}_2}{i_d} \tag{20}$$

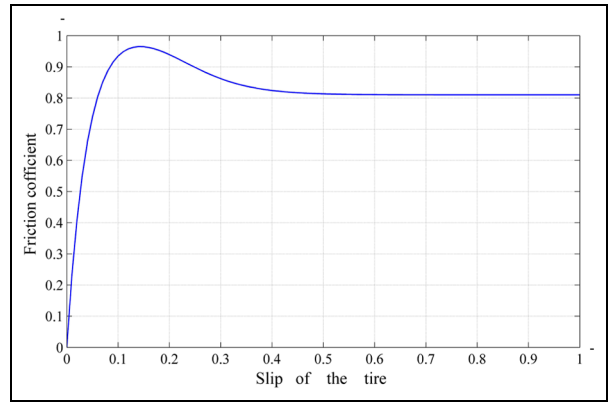

Figure 5. Tire characteristic.

$$T_2 \cdot i_d = -C_2(\dot{\theta}_8 - \dot{\theta}_t) - K_2(\theta_8 - \theta_t) \tag{21}$$

where θ_8 and θ_t are the rotational displacement of the drive shaft and the tire, respectively; i_d is the final ratio; K_2 is the equivalent stiffness coefficient of output shaft; and C_2 is the equivalent damping coefficient of output shaft.

The tire model calculates a slip from the drive shaft speed and the vehicle velocity, and interpolates a friction coefficient according to the prescribed slip characteristic which is a curve (Figure 5). The dynamic equations of the tire model are shown in equations (22) and (23)

$$\lambda = \begin{cases} (\dot{\theta}_t \cdot r - v)/\dot{\theta}_t \cdot r & \text{when skidding: } \dot{\theta}_t \cdot r \geq v \\ (v - \dot{\theta}_t \cdot r)/v & \text{when skidding: } \dot{\theta}_t \cdot r < v \end{cases} \tag{22}$$

$$I_t\ddot{\theta}_t + C_2(\dot{\theta}_8 - \dot{\theta}_t) + K_2(\theta_8 - \theta_t) = -F_t \cdot r \tag{23}$$

where λ is the tire slip; r is the tire radius; v is the vehicle velocity; I_t is the tire inertia; and F_t is the traction force.

The vehicle load model is established including grade resistance, aerodynamic drag, and rolling resistance. The dynamic equation of vehicle can be obtained (equation (24))

$$m\dot{v} = F_t - \left[mg\ \sin(\varphi) + \left(\frac{\rho A C_w v^2}{2 + mgf_r}\right)\right] \tag{24}$$

where m is the vehicle mass; g is the gravity acceleration; φ is the hill gradient angle; ρ is the air density; A is the effective vehicle area; C_w is the air drag coefficient; and f_r is the rolling resistance coefficient.

Principle of the four types of clutch-to-clutch shifts

The four basic types of clutch-to-clutch shifts are power-on upshift, power-on downshift, power-off upshift, and power-off downshift. When the torque is transferred from the input side to the output side of the transmission, the shift is called power-on shift; otherwise, the shift is called power-off shift. The shift processes of the four types can theoretically be divided into two phases which are torque phase and inertia phase, but the execution orders are different. The power-on upshift and power-off downshift go through the torque phase before the inertia phase; on the contrary, the power-on downshift and power-off upshift go through the inertia phase before the torque phase.

Before the analysis of the four basic types of clutch-to-clutch shifts, the concept of clutch's torque ability needs to be explained. For a clutch (Figure 2), the torque ability has two states (*True* or *False*) (equation (25))

$$Flag_{ta} = \begin{cases} True & (T_{ccd} > 0 \text{ and } \dot{\theta}_{cin} > \dot{\theta}_{cout}) \text{ or } (T_{ccd} < 0 \text{ and } \dot{\theta}_{cin} < \dot{\theta}_{cout}) \\ False & \text{else} \end{cases} \tag{25}$$

When the drive torque capacity is greater than zero and the input-side speed is faster than the output-side speed, or the drive torque capacity is less than zero and the input-side speed is slower than the output-side speed, the torque ability of the clutch is in *True* state; otherwise, the torque ability is in *False* state.

A simplified DCT-like diagram is used for principle analysis of clutch-to-clutch shift processes (Figure 6).

$$\Delta\dot{\theta}_{con} = \dot{\theta}_1 - \dot{\theta}_{on} \tag{26}$$

$$\Delta\dot{\theta}_{coff} = \dot{\theta}_1 - \dot{\theta}_{off} \tag{27}$$

$$T_{ccd} = T_1 - I_1 \cdot \ddot{\theta}_1 \tag{28}$$

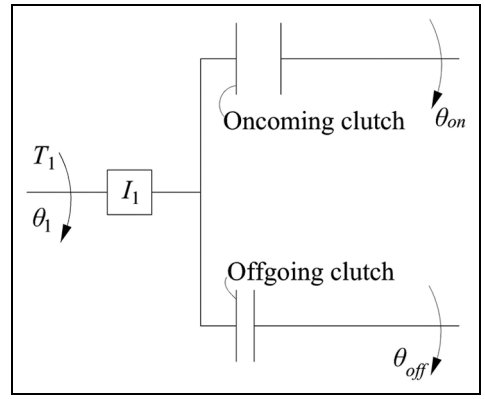

Figure 6. Schematic diagram for clutch-to-clutch shifts analysis.

where $\dot{\theta}_1$ is the turbine speed; $\dot{\theta}_{on}$ is the output-side speed of oncoming clutch; $\dot{\theta}_{off}$ is the output-side speed of offgoing clutch; $\Delta\dot{\theta}_{con}$ is the slip speed of oncoming clutch; $\Delta\dot{\theta}_{coff}$ is the slip speed of offgoing clutch; and T_{ccd} is the drive torque capacity of oncoming clutch and offgoing clutch.

Principle of power-on upshift

Power-on shift means the power is transferred from the input side to the output side of the transmission; therefore, the drive torque capacity of oncoming clutch (equation (28)) is greater than zero; because the gear ratio of the high gear is smaller than that of the low gear, the input-side speed of oncoming clutch is faster than the output-side speed, which means a positive slip speed (equation (26)). According to the definition above (equation (25)), the torque ability of oncoming clutch ($Flag_{ta}$) is in *True* state before the upshift. This can also be understood as that the oncoming clutch has the ability to "take over" the torque transferred by the offgoing clutch at this moment. Because of this, the first phase of power-on upshift is the torque phase, in which the torque will be transferred from the offgoing clutch to the oncoming clutch. As the capacity of oncoming clutch increases, the torque transferred by the offgoing clutch decreases automatically. When the actual torque of offgoing clutch reaches zero, the input torque has been handed over to oncoming clutch and then the torque phase should be finished. The next phase is the inertia phase. In the inertia phase, the gear ratio change occurs. The input-side speed of oncoming clutch should be decelerated in order to achieve synchronization with the target gear by several control methods. When the slip speed of oncoming clutch reaches zero, the inertia phase is finished and the shift is accomplished. The control principle of a power-on upshift is shown in Figure 7(a). Note that the engine torque is supposed to be constant except for the torque reduction during shift phase 3 (SP3) for the engine

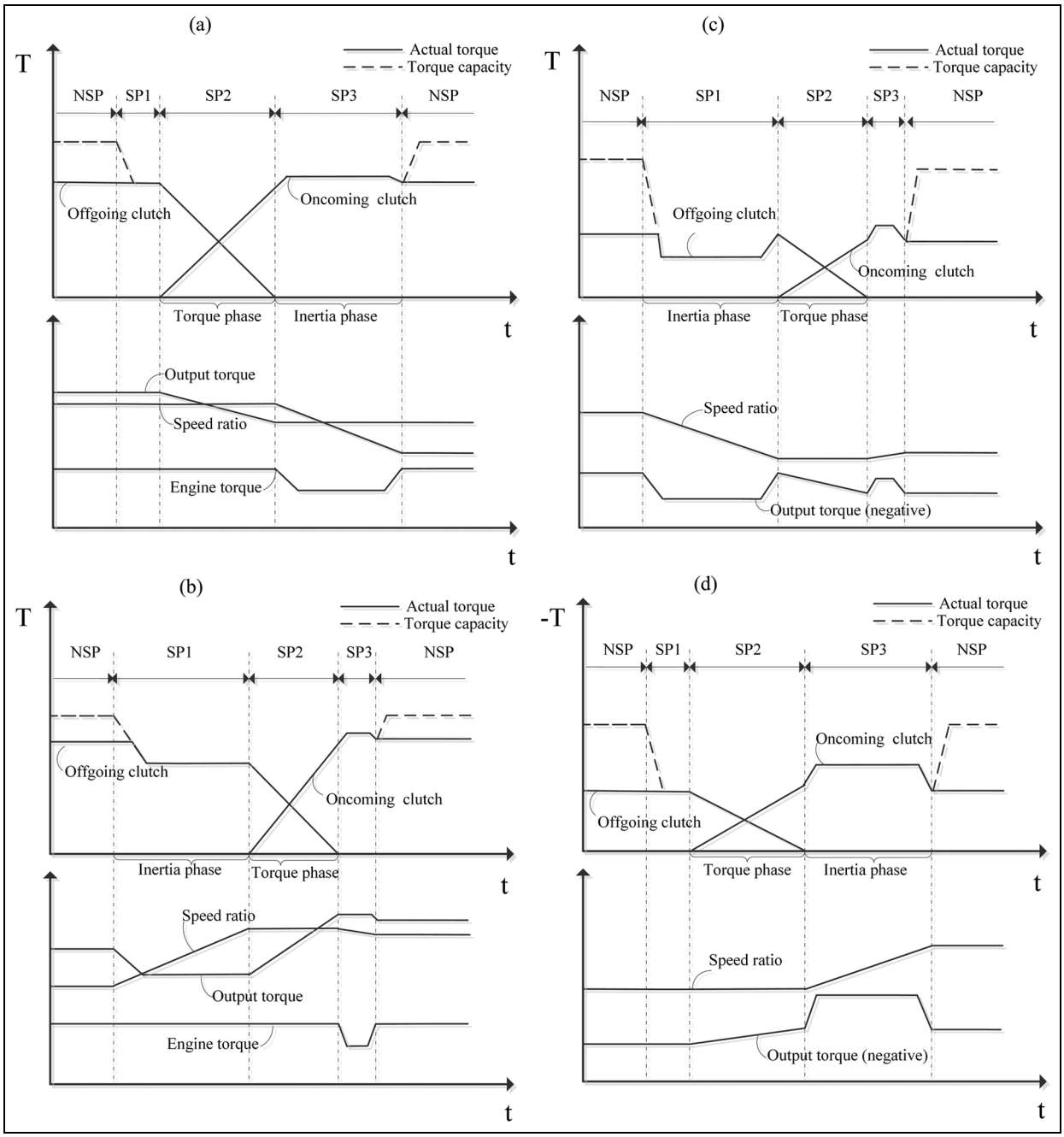

Figure 7. Control principle of the four types of clutch-to-clutch shifts: (a) power-on upshift, (b) power-off upshift, (c) power-on downshift, and (d) power-off downshift.

torque is input variable, which is determined primarily by the engine speed and throttle and could not be controlled by clutch-to-clutch shifts except for the torque reduction control. Note that the symbols in Figure 7 are descripted in the section "Generic control flow."

Principle of power-on downshift

Same with power-on upshift, the drive torque capacity of oncoming clutch is greater than zero, but because the gear ratio of the low gear is bigger than that of the high gear, the input-side speed of oncoming clutch is slower than the output-side speed. Therefore, the torque ability of oncoming clutch is in *False* state before the downshift process. This can also be understood as that the oncoming clutch do not have the ability to "take over" the torque transferred by the offgoing clutch at this moment. And thus the clutch-to-clutch torque-handover process should wait until the torque ability of oncoming clutch turns to *True* state. Because

of this, the first phase of power-on downshift is the inertia phase. In the inertia phase, the input-side speed of oncoming clutch should be accelerated in order to achieve synchronization with the target gear by several control methods. When the slip speed of oncoming clutch exceeds zero, the torque ability of oncoming clutch turns to *True* state and the inertia phase is finished. And then the torque phase begins in which the torque will be transferred from the offgoing clutch to the oncoming clutch. As the torque capacity of oncoming clutch increases, the torque capacity of offgoing clutch should be decreased by several control methods. When the actual torque of offgoing clutch reaches zero, the input torque has been handed over to oncoming clutch and the torque phase should be finished. Because a small slip speed of oncoming clutch may still exist, the downshift process may not get complete. Therefore, a short inertia phase is needed after the torque phase until the slip speed reaches zero. The control principle of a power-on downshift is shown in Figure 7(b).

Principle of power-off upshift

Power-off shift means the power is transferred from the output side to the input side of the transmission; thus, the drive torque capacity of oncoming clutch is less than zero, and the slip speed of oncoming clutch is positive. Therefore, the torque ability of oncoming clutch is in *False* state before the upshift. For the same reason with power-on downshift, the first phase of power-off upshift is the inertia phase. When the slip speed of oncoming clutch is controlled to be less than zero, the torque ability of oncoming clutch turns to *True* and then the inertia phase should be finished. The subsequent phase is the torque phase in which the negative torque will be transferred from the offgoing clutch to the oncoming clutch. When the actual torque of offgoing clutch reaches zero, the negative torque has been handed over to oncoming clutch and the torque phase should be finished. Like power-on downshift, a short inertia phase is needed after the torque phase until the slip speed reaches zero. The control principle of a power-off upshift is shown in Figure 7(c).

Principle of power-off downshift

The drive torque capacity of oncoming clutch is less than zero; the slip speed of oncoming clutch is negative. Therefore, the torque ability of oncoming clutch is in *True* state before the downshift. For the same reason with power-on upshift, the first phase of power-off downshift is the torque phase in which the negative torque will be transferred from the offgoing clutch to the oncoming clutch. When the actual torque of offgoing clutch reaches zero, the vehicle load has been handed over to the oncoming clutch and the torque phase should be finished. The second phase is the inertia phase. The input-side speed of oncoming clutch should be accelerated in order to achieve synchronization with the target gear. When the slip speed of oncoming clutch reaches zero, the inertia phase is finished and then the shift is accomplished. The power-off downshift principle is shown in Figure 7(d).

Frame of the shift controller

The shift controller of 6AT is designed with six parts (Figure 8). The execution sequence of them is shift schedule (SS), clutch role decision (CRD), GCF, virtual clutch information calculation (VCIC), oncoming virtual clutch controller (ONVCC), and offgoing virtual clutch controller (OFFVCC). Note that the algorithms of ONVCC and OFFVCC are exactly the same, but the input signals are different.

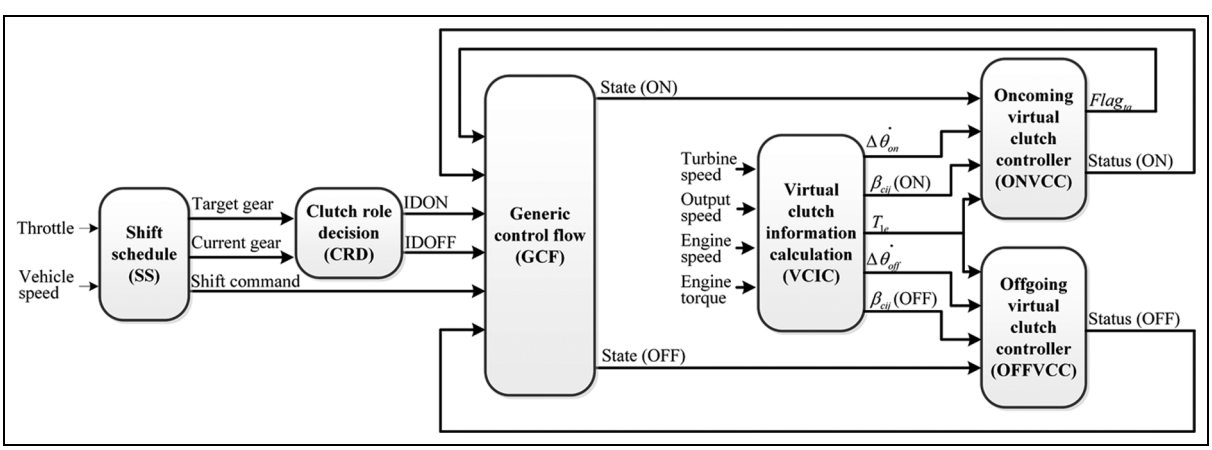

Figure 8. Frame of the shift controller of 6AT.

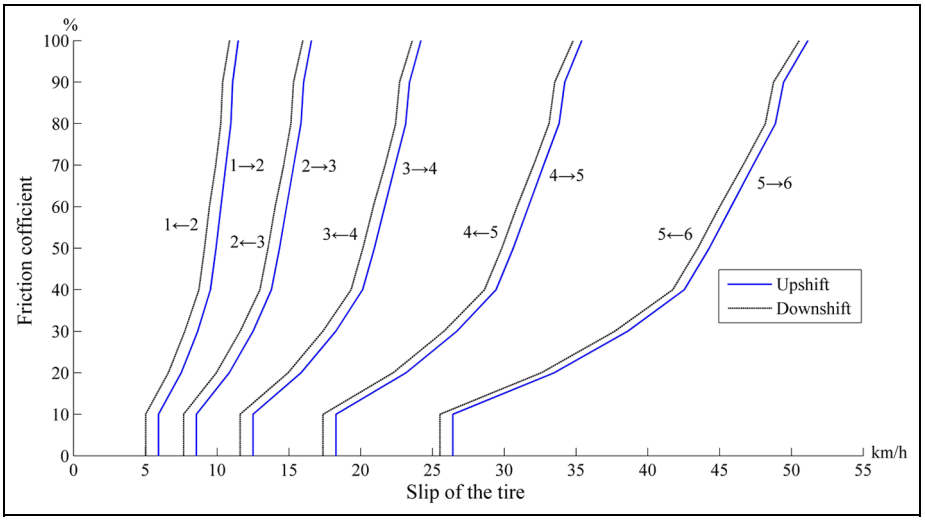

Figure 9. Shift schedule of 6AT.

Table 1. Use of shift elements.

Gear	C1	C2	C3	C4	C5	C6
D1	√	X	X	√	X	X
D2	X	√	X	√	X	X
D3	X	X	√	√	X	X
D4	√	X	X	X	√	X
D5	X	√	X	X	√	X
D6	X	X	√	X	√	X
R1	√	X	X	X	X	√
R2	X	√	X	X	X	√
R3	X	X	√	X	X	√

Shift schedule

The functionality of SS is to determine whether a clutch-to-clutch shift process should be carried out. A new vehicle intelligent shift system is proposed by Hui and Anlin,[18] but only the two-parameter SS based on throttle and vehicle speed is adopted in this study for simplicity (Figure 9). The estimated vehicle speed can be calculated by the output speed of 6AT (equation (29))

$$v_e = \frac{\dot{\theta}_2 \cdot r}{i_d} \tag{29}$$

where v_e is the estimated vehicle speed.

For example, if a 1-2 upshift is to be carried out, the target gear is D2 and the current gear is D1.

CRD

The functionality of CRD is to determine the ID of oncoming clutch (IDON) and the ID of offgoing clutch (IDOFF) according to the use of shift elements (Table 1). For example, if the target gear is D2 and the current gear D1, IDON is C2 and IDOFF is C1.

Virtual clutch controller

In order to simplify the algorithms of the shift controller, the ONVCC is designed exactly the same with the OFFVCC, and both of them are commanded by the upper controller, that is, the GCF. ONVCC, and OFFVCC are designed with eight states, that is, engage state (ES), disengage state (DS), fill state (FS), micro slip state (MSS), oncoming torque state (ONTS), offgoing torque state (OFFTS), oncoming inertia state (ONIS), and offgoing inertia state (OFFIS) (Figure 10).

In ES, the object is to keep the torque capacity of the clutch always larger than the drive torque capacity to ensure the clutch is in stick state. In DS, the object is to keep the torque capacity equivalent to zero to ensure no torque is transferred by the clutch. In FS, the object is to make sure the clearance in the oil line of oncoming clutch is filled up, but the actual torque of the clutch

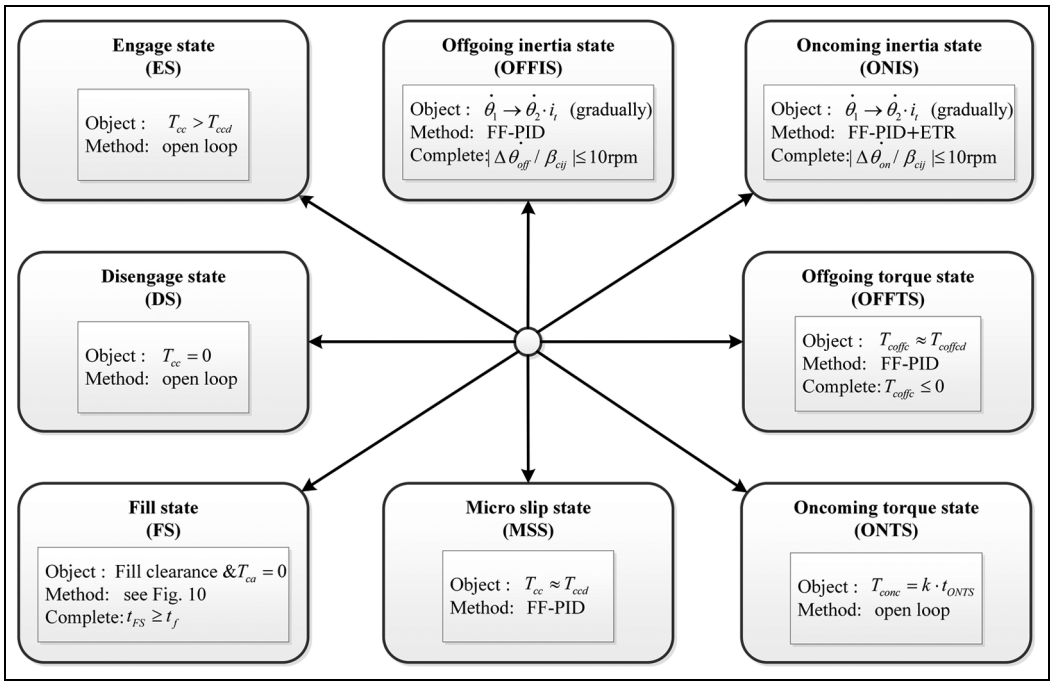

Figure 10. Virtual clutch controller.

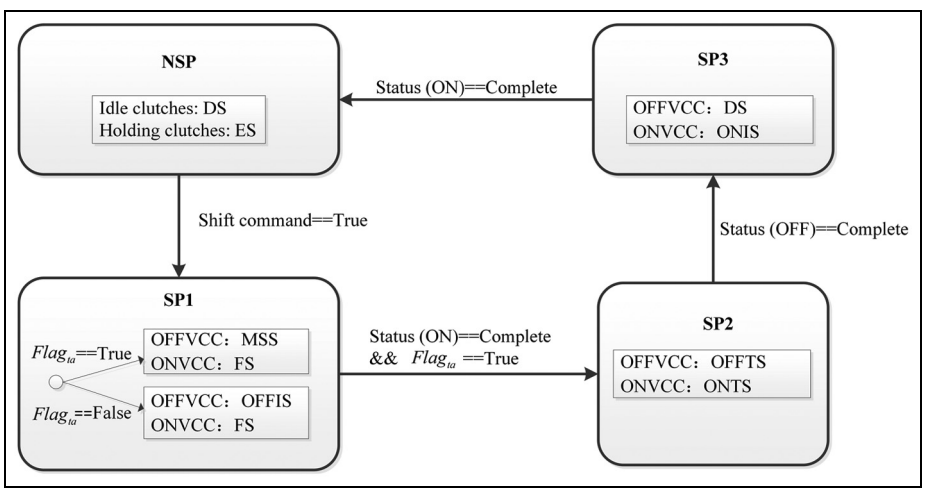

Figure 11. Schematic diagram of the generic control flow.

remains at zero. In MSS, the object is to keep the torque capacity of the clutch equivalent to the drive torque capacity. In ONTS, the object is to increase the actual torque of oncoming clutch to follow a slope in order to take over the torque from offgoing clutch smoothly. In OFFTS, the object is to keep torque capacity equivalent to the drive torque capacity of offgoing clutch. In ONIS, the object is to control the turbine speed to reach the target gear speed level gradually in the inertia phase after torque phase. In OFFIS, the object is to control the turbine speed to reach the target gear speed level gradually in the inertia phase before torque phase.

Generic control flow

The functionality of GCF is to manage overall process flow for clutch-to-clutch shifts, and command the lower controllers, that is, ONVCC and OFFVCC, to carry out related control algorithms. According to the principle analysis of the four types of clutch-to-clutch shifts,

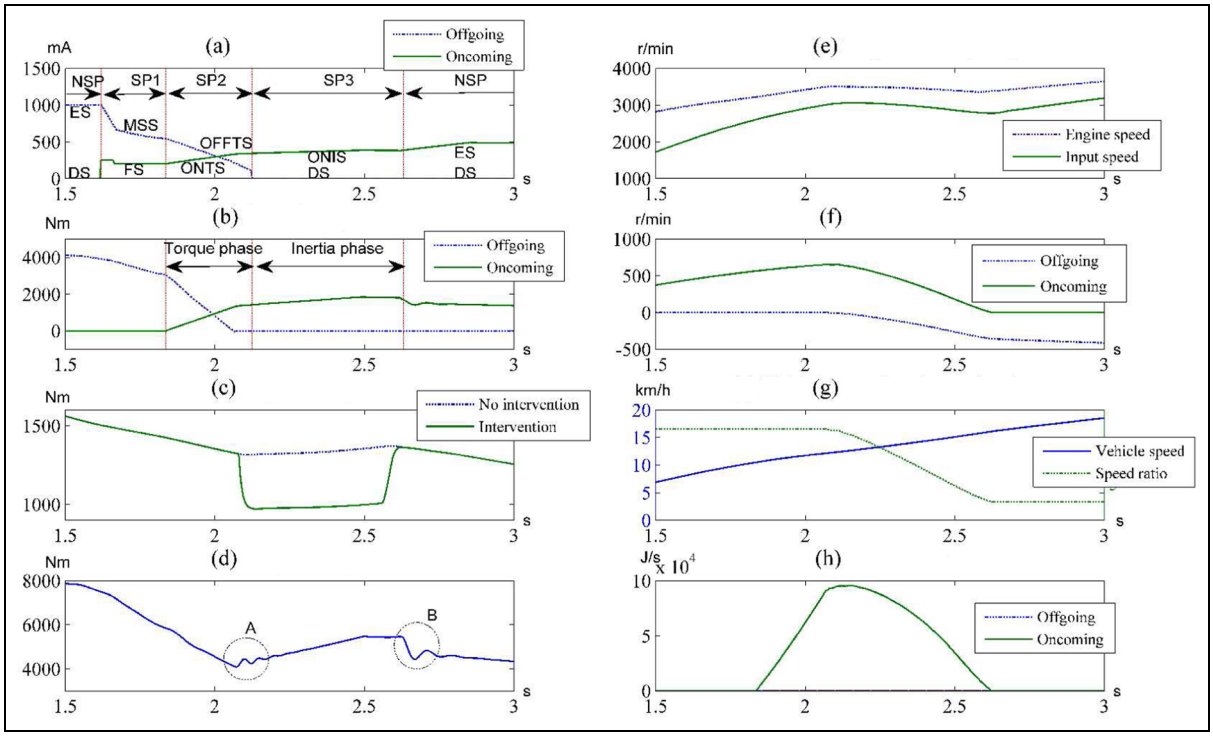

Figure 12. Power-on upshift from D1 to D2 gear: (a) control current, (b) actual torque, (c) engine torque, (d) output torque, (e) engine speed and input speed, (f) slip speed, (g) vehicle speed and speed ratio, and (h) slip power.

the GCF is designed with four phases, that is, no shift phase (NSP), shift phase 1 (SP1), shift phase 2 (SP2), and SP3 (Figure 11). The four phases are also denoted in Figure 7.

The first phase is NSP. There is no shift demand needed to be executed in this phase, and thus, the torque capacity of the holding clutches, such as C1 and C4 for the D1 gear (Table 1), should larger than the drive torque capacity to ensure these clutches are in stick states. Therefore, the holding clutches is set to ES, and the others is set to DS. When a clutch-to-clutch shift command is sent from the SS, the GCF enters SP1.

It is known that power-on upshift and power-off downshift go through the torque phase before the inertia phase, and power-on downshift and power-off upshift go through the inertia phase before the torque phase. Through the previous principle analysis, a fundamental rule can be summarized which is that the clutch-to-clutch "torque-handover" process, that is, the torque phase is based on the condition that the oncoming clutch has the ability to take over the torque transferred by the offgoing clutch. Two conditions should be satisfied to achieve the ability, one is that the torque ability of oncoming clutch is in *True* state and the other is that the fill process of oncoming clutch is complete. Therefore, the object of SP1 is designed to ensure the oncoming clutch has this ability for the following torque phase.

Therefore, when the GCF is entering SP1, if the torque ability of oncoming clutch is in *True* state, the OFFVCC is set to MSS to keep the offgoing clutch ready for the torque phase, and the ONVCC is set to FS to fill the clearance. When the fill process of oncoming clutch is complete, the object of SP1 is complete and the GCF enters SP2; if the torque ability of oncoming clutch is in *False* state, the OFFVCC is set to OFFIS to control the turbine speed to reach the target gear speed level, and ONVCC is also set to FS. When the torque ability of oncoming clutch turns to *True* state and the fill process of oncoming clutch is complete, the GCF enters SP2.

The object of SP2 is designed to carry out the clutch-to-clutch "torque-handover" process smoothly. In SP2, the OFFVCC is set to OFFTS and the ONVCC is set to ONTS, and thus, the torque transferred by the offgoing clutch begins to transfer to the oncoming clutch. When the actual torque of offgoing clutch reaches zero which means the torque transferred by offgoing clutch has all been handed over to the oncoming clutch, the status of OFFVCC turns to complete status and then the GCF enters SP3.

Because the torque phase has happened in SP2, the torque is transferred to the oncoming clutch. In order to reduce the slip power generated at the oncoming clutch and improve smoothness, the object of SP3 is to reduce the slip speed of oncoming clutch gradually until

to a small slip (10 r/min), and SP3 can also be understood as the inertia phase after torque phase. Therefore, the OFFVCC is set to DS to ensure no torque is transferred by the offgoing clutch, and the ONVCC is set to ONIS to reduce the slip speed of oncoming clutch. When the slip speed of oncoming clutch approaches to zero, the inertia phase is complete and ONVCC turns to complete status. Then, the GCF gets back to NSP. The clutch-to-clutch shift is complete in the meantime.

Shift control results and analysis

Power-on upshift

Based on the GCF for the four types of clutch-to-clutch shifts, a power-on upshift from D1 to D2 gear is simulated (Figure 12) at a vehicle speed of around 7 km/h and wide-open-throttle (WOT). Note that the simulation results are based on a heavy duty truck, the vehicle weight is around 35,000 kg and the maximum engine torque is around 2800 N m. The offgoing clutch is C1 and the oncoming clutch is C2 (Table 1). The diagram consists of eight graphs: Figure 12(a) shows the control current sent to the solenoids of offgoing clutch and oncoming clutch; the four phases of the GCF and the states of the OFFVCC and the ONVCC are also indicated in this figure; Figure 12(b) pictures the actual torques of offgoing clutch and oncoming clutch and the processes of torque phase and inertia phase; Figure 12(c) shows the engine torque without intervention and the engine torque with intervention; Figure 12(d) shows the output torque of 6AT; Figure 12(e) shows the engine speed and the turbine speed; Figure 12(f) shows the slip speed of offgoing clutch and the slip speed of oncoming clutch; and Figure 12(g) shows the vehicle speed and the speed ratio of the transmission. The 1-2 upshift starts at 1.6 s and ends at around 2.6 s.

Before the clutch-to-clutch shift process, the GCF is in NSP; therefore, the holding clutches (C1 and C4) are in ES and the idle clutches (C2, C3, C5, and C6) are in DS (Figure 12(a)). When the SS determines a shift command according to Figure 9, the GCF enters SP1, and then the clutch-to-clutch shift process begins. At this time, the drive torque capacity of C2 is greater than 0 and the slip speed of C2 is positive (Figure 12(f)), and thus the torque ability of oncoming clutch is in *True* state. Therefore, the OFFVCC is in MSS and the ONVCC is in FS according to Figure 11. During SP1, the torque capacity of offgoing clutch is reduced gradually to the actual torque level, and the oncoming clutch is in fill process. Note that the declines of the actual torque of offgoing clutch and the output torque of the transmission are not caused by the control of MSS, but by the decline of the engine torque due to the increase in the engine speed (Figure 12(b), (c) and (e)).

When the fill time of oncoming clutch is up, the GCF enters SP2. During SP2, the OFFVCC is in OFFTS and the ONVCC is in ONTS; therefore, the torque phase begins. The actual torque of oncoming clutch increases gradually, and the actual torque of offgoing clutch decreases by feed-forward and proportional–integral–derivative (FF-PID) control. The output torque decreases faster than the engine torque in the torque phase (Figure 12(d)), because the torque transferred by the low gear is transferring to the high gear. The slip power of oncoming clutch begins to increase due to the increase in its actual torque.

The torque capacity of offgoing clutch decreases to zero at around 2.1 s, and thus, the input torque has been handed over to the oncoming clutch, and then the GCF enters SP3. During SP3, the OFFVCC is in DS and the ONVCC is in ONIS; therefore, the inertia phase begins. The engine torque reduction control is executed at the beginning of SP3 (Figure 12(c)), and the FF-PID control is also used to track a desired trajectory of the turbine speed. Therefore, the speed ratio of 6AT (Figure 12(g)) begins to decrease, and the turbine speed and the engine speed also start to decrease to the D2 gear level. Note that the small vibration of output torque (dashed circle A in Figure 12(d)) is mainly caused by the transition of engine torque which stops decreasing and starts to increase due to the transition of engine speed (Figure 12(c)–(e)). During SP3, due to the combined effect of engine torque reduction and FF-PID controlled by ONIS, the turbine speed and speed ratio change smoothly. In addition, because the engine torque reduction control plays a leading role for the speed change, there is only a small "hump" of output torque and the slip power of oncoming clutch is also reduced. When the slip speed of oncoming clutch (Figure 12(f)) reaches 0 r/min, the engine torque with intervention begins to return to the level of engine torque without intervention (Figure 12(c)).

When the slip speed of oncoming clutch is smaller than 10 r/min, the GCF gets back to NSP, and then the control current of C2 increases to a high level gradually, and the power-on upshift process is finished. Note that the vibration of output torque (dashed circle B in Figure 12(d)) is caused by the stick-slip phenomenon of C2.

During the upshift process, the output torque follows the engine torque well; thus, the vehicle speed is barely affected by the shift (Figure 12(g)). Other simulations with different initial conditions (different vehicle speed, different throttle, and different gear) of power-on upshifts are also run and show good shift performance based on the GCF.

Power-on downshift

Figure 13 displays a power-on downshift from D3 to D2 gear at a vehicle speed of around 20 km/h and

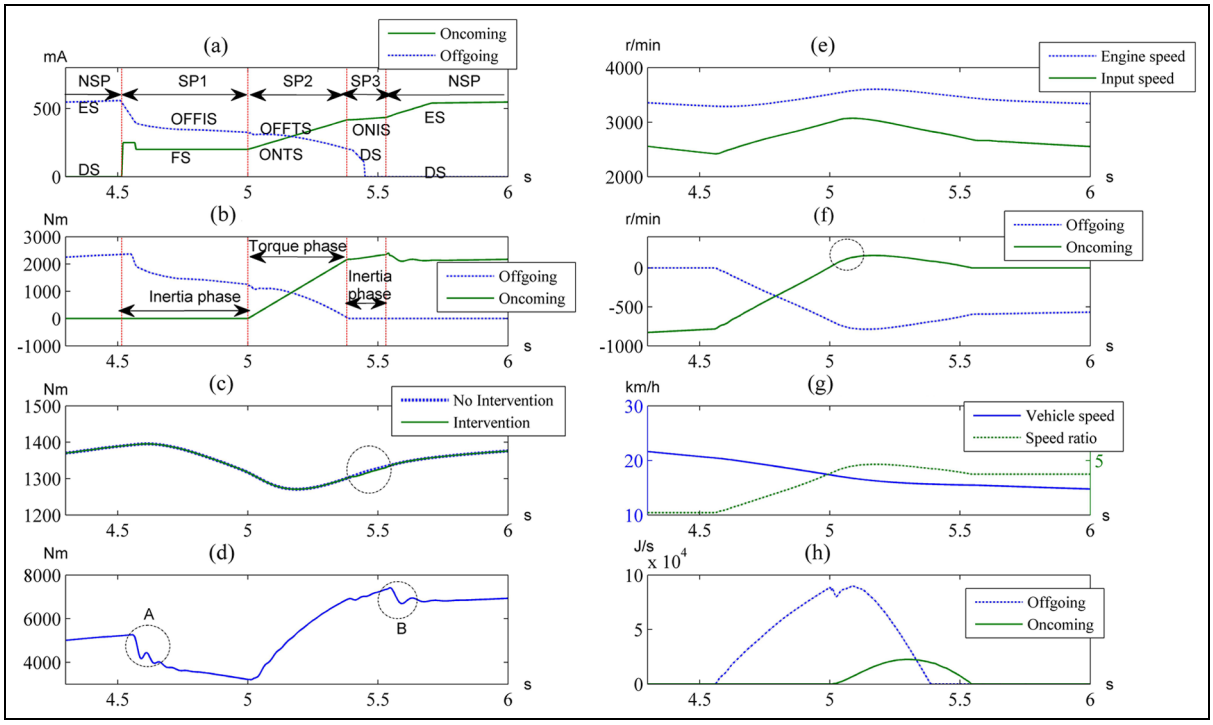

Figure 13. Power-on downshift from D3 to D2 gear: (a) control current, (b) actual torque, (c) engine torque, (d) output torque, (e) engine speed and input speed, (f) slip speed, (g) vehicle speed and speed ratio, and (h) slip power.

WOT. The layout of Figure 13 is the same as Figure 12. The 3-2 downshift starts at 4.5 s and ends at around 5.6 s.

Before the shift process, the GCF is in NSP; therefore, the holding clutches (C3 and C4) are in ES and the idle clutches (C1, C2, C5, and C6) are in DS. The vehicle is running at a road grade of 20°; therefore, the vehicle speed decreases, and a downshift is necessary to increase the output torque.

The SS determines a shift command at around 4.5 s; thus, the GCF enters SP1. At this time, because the drive torque capacity of oncoming clutch is positive and the slip speed of oncoming clutch is negative (Figure 13(f)), the torque ability of C3 is in *False* state. Therefore, the OFFVCC is in OFFIS and the ONVCC is in FS. During SP1, the inertia phase begins. The torque capacity of offgoing clutch reduces to a low level in order to provide sufficient inertia torque for the input speed to increase following a desired curve (Figure 13(e)) by FF-PID control, and the oncoming clutch is in fill process. Note that if the engine torque is controlled to increase, the drop of the output torque (dashed circle A in Figure 13(d)) can be avoided, but it could lead to a higher slip power of offgoing clutch during the inertia phase.

The slip speed of oncoming clutch turns to positive at around 5 s (Figure 13(f)), and then the torque ability of C2 turns to *True* state, and thus the GCF enters SP2. During SP2, the OFFVCC is in OFFTS and the ONVCC is in ONTS. Therefore, same with SP2 of power-up shift, the torque phase begins. Note that the output torque increases faster than the engine torque, because the torque transferred by the high gear is transferring to the low gear (Figure 13(d)), and the increase in slip speed of oncoming clutch at the beginning of torque phase (dashed circle in Figure 13(f)) can be reduced by increasing the torque capacity of offgoing clutch, but it could lead to a spurt of output torque and a higher slip power because of the high slip speed of offgoing clutch.

The torque capacity of offgoing clutch decreases to zero at around 5.4 s, and then the GCF enters SP3. Although the slip speed of oncoming clutch reduces gradually, it is still higher than 10 r/min. Therefore, a short inertia phase is necessary to synchronize the oncoming clutch. During SP3, the OFFVCC is in DS and the ONVCC is in ONIS; thus, the control strategy is the same as SP3 of power-on upshift. The engine torque reduction (dashed circle in Figure 13(c)) is small because of the small slip speed of oncoming clutch.

Soon the slip speed of oncoming clutch becomes smaller than 10 r/min, and then the GCF gets back to NSP, and then the control current of oncoming clutch increases to a high level gradually, and the power-on downshift process is finished. Note that the vibration of output torque (dashed circle B in Figure 13(d)) is caused by the stick-slip phenomenon of oncoming clutch.

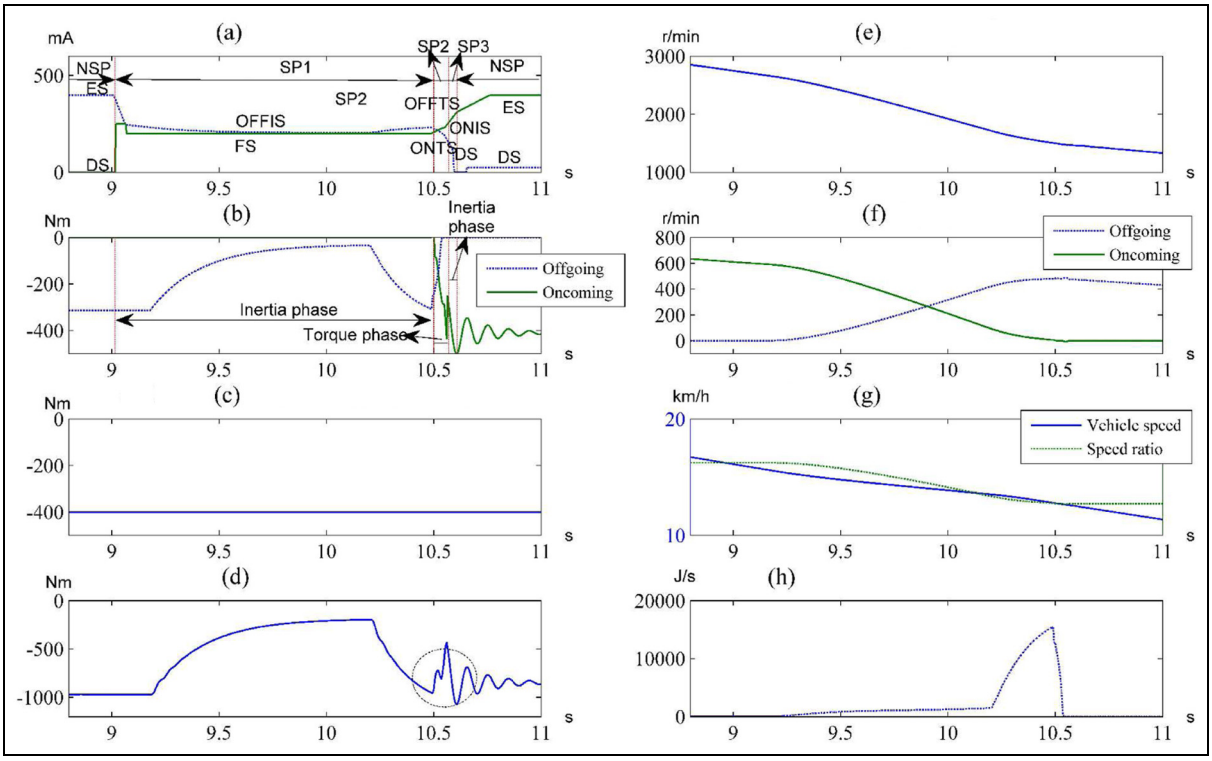

Figure 14. Power-off upshift from D2 to D3 gear: (a) control current, (b) actual torque, (c) engine torque without intervention, (d) output torque, (e) input speed, (f) slip speed, (g) vehicle speed and speed ratio, and (h) slip power of offgoing clutch.

During the downshift process, the speed ratio (Figure 13(g)) and the output torque (Figure 13(d)) change from the high gear level to the low gear level similar to the desired trajectory (Figure 7(b)), and the deceleration of vehicle speed is reduced gradually. Other simulations of different initial conditions of power-on downshifts are also run and present good shift performance based on the GCF.

Power-off upshift

Figure 14 pictures a power-off upshift from D2 to D3 gear at a vehicle speed of around 16 km/h and 0% throttle. The layout of Figure 14 is the same as Figure 12. The 2-3 upshift starts at 9 s and ends at around 10.6 s.

Before the shift process, the GCF is in NSP; therefore, the holding clutches (C2 and C4) are in ES and the idle clutches (C1, C3, C5, and C6) are in DS. Because the throttle opening is 0%, the engine stops generating power. And the drag torque of the engine and accessories is around −400 N m; therefore, the power is transferred from the output side of 6AT to the input side and the vehicle is slowing down (Figure 14(g)).

The SS determines a shift command at around 9 s; thus, the GCF enters SP1. At this time, the drive torque capacity of oncoming clutch is negative and the slip speed of oncoming clutch is positive, and thus, the torque ability of oncoming clutch is in *False* state. Therefore, the OFFVCC is in OFFIS and the ONVCC is in FS.

According to the GCF, the state flows of the ONVCC and the OFFVCC of power-off upshift are the same to that of power-on downshift, and thus, the control methods of them are similar. Some differences need to be explained. Because the torque is transferred from the output side to the input side of the transmission, releasing the offgoing clutch in OFFIS can reduce the slip speed of the oncoming clutch; engine torque reduction control is not used in ONIS. Note that the duration time of the SP1 in Figure 14(a) is longer than that in Figure 13(a), because only the small drag torque can be used to decrease the turbine speed in the inertia phase of power-off shift. Note that the continuous wave of the actual torque of the oncoming clutch and the output torque (dashed circle in Figure 14(d)) is caused by the stick-slip phenomenon of oncoming clutch.

During the upshift process, no torque interruption occurs, and the speed ratio (Figure 14(g)) and the output torque (Figure 14(d)) change from the low gear level to the high gear level with expectations. Other simulations of different initial conditions of power-off upshifts are also run and present good shift performance based on the GCF.

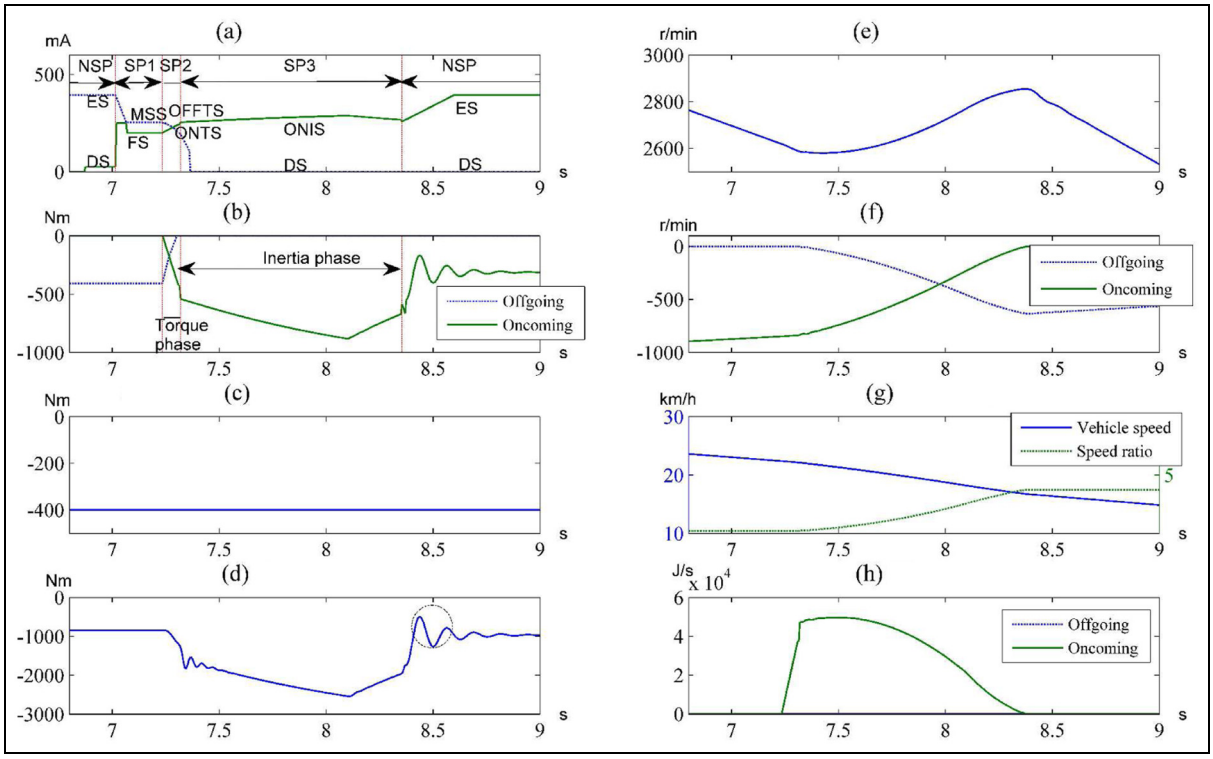

Figure 15. Power-off downshift from D3 to D2 gear: (a) control current, (b) actual torque, (c) engine torque without intervention, (d) output torque, (e) input speed, (f) slip speed, (g) vehicle speed and speed ratio, and (h) slip power.

Power-off downshift

Figure 15 pictures a power-off downshift from D3 to D2 gear at a vehicle speed of around 23 km/h and 0% throttle. The layout of Figure 15 is the same as Figure 12. The 3-2 downshift starts at 7 s and ends at around 8.4 s.

Before the shift process, the GCF is in NSP; therefore, the holding clutches (C3 and C4) are in ES and the idle clutches (C1, C2, C5, and C6) are in DS. Same with power-off upshift, the power is transferred from the output side of 6AT to the input side and the vehicle is slowing down (Figure 15(g)).

The SS determines a shift command at around 7 s; thus, the GCF enters SP1. At this time, the drive torque capacity of oncoming clutch is negative and the slip speed of oncoming clutch is negative (Figure 15(f)), and thus, the torque ability of oncoming clutch is in *True* state. Therefore, the OFFVCC is in MSS and the ONVCC is in FS.

According to the GCF, the state flows of the ONVCC and the OFFVCC of power-off downshift are the same as that of power-on upshift, and thus, the control methods of them are similar. Note that because the engine torque reduction control cannot be used in ONIS, the duration time of the SP3 in Figure 15(a) is longer than that in Figure 12(a), and there is an inverted "hump" in the actual torque of the oncoming clutch and the output torque during the inertia phase.

During the power-off downshift process, no torque interruption occurs, and the speed ratio (Figure 15(g)) and the output torque (Figure 15(d)) change from the low gear level to the high gear level with expectations. Other simulations of different initial conditions of power-off downshifts are also run and present good shift performance based on the GCF.

Conclusion

In the article, the principle of four types of clutch-to-clutch shifts is analyzed in detail. A fundamental rule is summarized that the clutch-to-clutch "torque-handover" process, that is, the torque phase, of the four types is based on the condition that the oncoming clutch has the ability to take over the torque transferred by the offgoing clutch. Thus, the concept of oncoming clutch's torque ability is proposed. A GCF for the clutch-to-clutch shifts is designed with four phases to simplify the control algorithms in TCU. In the SP1, the object is to make the oncoming clutch has the ability to take over the torque. In the SP2, the object is to carry out the clutch-to-clutch "torque-handover" process smoothly. In the SP3, the object is to

reduce the slip speed of oncoming clutch gradually until to a small slip. With the powertrain model based on a heavy duty truck, the GCF is verified by software-in-the-loop simulations.

Declaration of conflicting interests

The author(s) declared no potential conflicts of interest with respect to the research, authorship, and/or publication of this article.

Funding

The author(s) disclosed receipt of the following financial support for the research, authorship, and/or publication of this article: The Innovation Foundation of BUAA for PhD Graduates (BY1213114), the Beijing Key Laboratory for High-efficient Power Transmission and System Control of New Energy Resource Vehicle, the Transformation Project of Independent Innovation Achievements in Shandong Province (2014CGZH1001), the Natural Science Foundation of Shandong Province (BS2015ZZ007), and the National Natural Science Foundation of China (51405010).

References

1. Runde JK. *Modelling and control of an automatic transmission*. Master's Thesis, Massachusetts Institute of Technology, Cambridge, MA, 1986.
2. Yoon A and Khargonekar P. Randomized algorithms for open-loop control of clutch-to-clutch transmissions. *J Dyn Syst: T ASME* 1999; 121: 508–517.
3. Haj-Fraj A and Pfeiffer F. A model based approach for the optimisation of gearshifting in automatic transmissions. *Int J Vehicle Des* 2002; 28: 171–188.
4. Bai S, Moses RL, Schanz T, et al. Development of a new clutch-to-clutch shift control technology. SAE paper 2002-01-1252, 2002.
5. Kim D, Yang K, Hong K, et al. Smooth shift control of automatic transmissions using a robust adaptive scheme with intelligent supervision. *Int J Vehicle Des* 2003; 32: 250–272.
6. Goetz M, Levesley MC and Crolla DA. Integrated powertrain control of gearshifts on twin clutch transmissions. SAE paper 2004-01-1637, 2004.
7. Kulkarni M, Shim T and Zhang Y. Shift dynamics and control of dual-clutch transmissions. *Mech Mach Theory* 2007; 42: 168–182.
8. Dong P, Liu Y and Xu X. A method of applying two-pump system in automatic transmissions for energy conservation. *Adv Mech Eng* 2015; 7: 1–11.
9. Walker PD, Zhang N and Tamba R. Control of gear shifts in dual clutch transmission powertrains. *Mech Syst Signal Pr* 2011; 25: 1923–1936.
10. Walker PD and Zhang N. Modelling of dual clutch transmission equipped powertrains for shift transient simulations. *Mech Mach Theory* 2013; 60: 47–59.
11. Goetz M, Levesley MC and Crolla DA. Dynamics and control of gearshifts on twin-clutch transmissions. *Proc IMechE, Part D: J Automobile Engineering* 2005; 219: 951–963.
12. Liu Y, Jiang H, Zhang Y, et al. A systematic model for dynamics and control of dual clutch transmissions. *J Mech Design* 2009; 131: 61012–61018.
13. Liu Y, Qin D, Jiang H, et al. Shift control strategy and experimental validation for dry dual clutch transmissions. *Mech Mach Theory* 2014; 75: 41–53.
14. Bai S, Maguire J and Peng H. *Dynamic analysis and control system design of automatic transmissions*. Warrendale, PA: Society of Automotive Engineers, 2013.
15. Society of Automotive Engineers. *Design practices: passenger car automatic transmissions*. 3rd ed. Warrendale, PA: Society of Automotive Engineers, 1994, p.18.
16. Song M, Oh J, Choi S, et al. Optimal line pressure control for an automatic transmission-based parallel hybrid electric vehicle considering mode change and gear shift. *Adv Mech Eng* 2014; 6: 216098.
17. Xie CF, Wang Q, Cheng Y, et al. *Dynamics*. Beijing, China: Higher Education Press, 2004, pp.140–160.
18. Hui J and Anlin G. A new vehicle intelligent shift system. *Adv Mech Eng* 2013; 5: 303691.